Research article JHEP|Reports

Transcriptomic analysis across liver diseases reveals disease-modulating activation of constitutive androstane receptor in cholestasis

Authors

Bhoomika Mathur, Waqar Arif, Megan E. Patton, Rahiman Faiyaz, Jian Liu, Jennifer Yeh, Sanjiv Harpavat, Kristina Schoonjans, Auinash Kalsotra, Antony M. Wheatley, Sayeepriyadarshini Anakk

Correspondence

anakk@illinois.edu (S. Anakk).

Graphical abstract

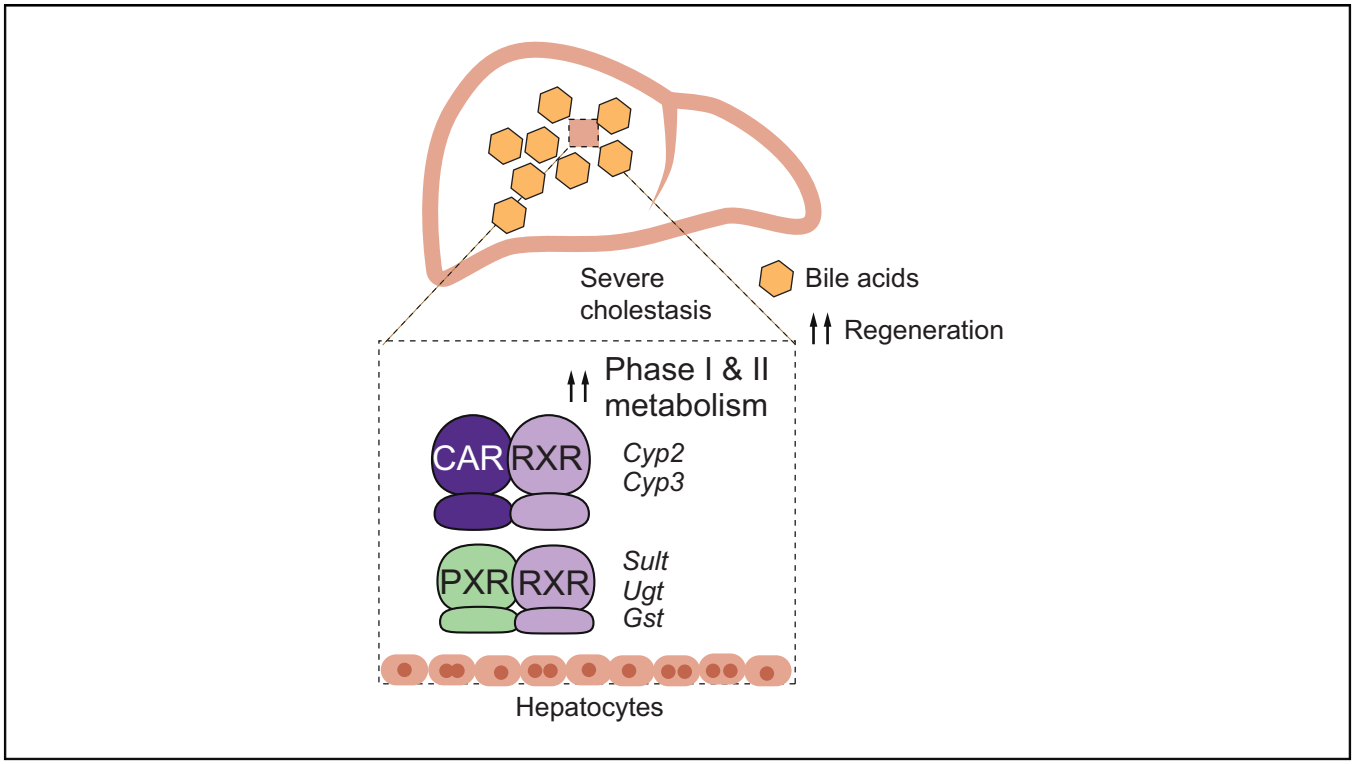

Highlights

- Cell cycle, inflammation, and glucose homeostasis are some of the common pathways altered in a variety of liver disorders.
- Phase I and II metabolic genes are induced in *Fxr*$^{-/-}$*Shp*$^{-/-}$ double knockouts (DKOs) and bile-acid-fed control mice.
- Activation of xeno-sensor, constitutive androstane receptor (CAR), is observed in cholestasis.
- Inhibiting CAR activity in DKO mice exacerbates zoxazolamine-induced paralysis and acetaminophen-induced hepatotoxicity.
- A subset of patients with biliary atresia display increased expression of CAR target protein CYP2B6.

Lay summary

Transcriptomic analysis of diverse liver diseases revealed alterations in common and distinct pathways. Specifically, in cholestasis, we found that detoxification genes and their activity are increased. Thus, cholestatic patients may have an unintended consequence on drug metabolism and not only have a beneficial effect against liver toxicity, but also may require adjustments to their therapeutic dosage.

https://doi.org/10.1016/j.jhepr.2020.100140

Research article

JHEP|Reports

Transcriptomic analysis across liver diseases reveals disease-modulating activation of constitutive androstane receptor in cholestasis

Bhoomika Mathur,[1] Waqar Arif,[2] Megan E. Patton,[1] Rahiman Faiyaz,[3] Jian Liu,[1] Jennifer Yeh,[4] Sanjiv Harpavat,[4] Kristina Schoonjans,[5] Auinash Kalsotra,[2] Antony M. Wheatley,[3] Sayeepriyadarshini Anakk[1,*]

[1]*Department of Molecular and Integrative Physiology, University of Illinois at Urbana-Champaign, Urbana, IL, USA;* [2]*Department of Biochemistry, University of Illinois at Urbana-Champaign, Urbana, IL, USA;* [3]*Department of Physiology, School of Medicine, National University of Ireland, Galway, Ireland;* [4]*Department of Pediatrics, Texas Children's Hospital, Houston, TX, USA;* [5]*Institute of Bioengineering, École Polytechnique Fédérale de Lausanne, Lausanne, Switzerland*

JHEP Reports **2020.** https://doi.org/10.1016/j.jhepr.2020.100140

Background & Aims: Liver diseases are caused by many factors, such as genetics, nutrition, and viruses. Therefore, it is important to delineate transcriptomic changes that occur in various liver diseases.
Methods: We performed high-throughput sequencing of mouse livers with diverse types of injuries, including cholestasis, diet-induced steatosis, and partial hepatectomy. Comparative analysis of liver transcriptome from mice and human samples of viral infections (HBV and HCV), alcoholic hepatitis (AH), non-alcoholic steatohepatitis (NASH), and biliary atresia revealed distinct and overlapping gene profiles associated with liver diseases. We hypothesised that discrete molecular signatures could be utilised to assess therapeutic outcomes. We focused on cholestasis to test and validate the hypothesis using pharmacological approaches.
Results: Here, we report significant overlap in the expression of inflammatory and proliferation-related genes across liver diseases. However, cholestatic livers were unique and displayed robust induction of genes involved in drug metabolism. Consistently, we found that constitutive androstane receptor (CAR) activation is crucial for the induction of the drug metabolic gene programme in cholestasis. When challenged, cholestatic mice were protected against zoxazolamine-induced paralysis and acetaminophen-induced hepatotoxicity. These protective effects were diminished upon inhibition of CAR activity. Further, drug metabolic genes were also induced in the livers from a subset of biliary atresia patients, but not in HBV and HCV infections, AH, or NASH. We also found a higher expression of CYP2B6, a CAR target, in the livers of biliary atresia patients, underscoring the clinical importance of our findings.
Conclusions: Comparative transcriptome analysis of different liver disorders revealed specific induction of phase I and II metabolic genes in cholestasis. Our results demonstrate that CAR activation may lead to variations in drug metabolism and clinical outcomes in biliary atresia.

Introduction

The liver plays a fundamental role in drug metabolism and detoxification. Multiple factors, including genetics, diet, alcohol, and viral infections, can compromise its function. For instance, cholestatic liver disease can be induced by drugs, secondary to mutations, or caused by immune modulation.[1–3] High-fat and Western diet primarily drive the development of fatty liver disease and non-alcoholic steatohepatitis (NASH), whereas excessive alcohol consumption and hepatitis B and C infections can lead to cirrhosis and eventually to cancer. As different therapeutic interventions are employed to treat these conditions, it is essential to understand the molecular networks perturbed during these disease states.

Here, we used high-throughput sequencing to analyse different liver diseases to identify their common and distinct gene signatures. We generated transcriptome data from mouse models of cholestasis, diet-induced fatty liver disease, and liver regeneration following partial hepatectomy (PHx). We anticipated that liver function would be compromised during diseased states resulting in reduced metabolic capacity.

However, confounding liver metabolic function data have been reported in the context of primary biliary cirrhosis, liver cirrhosis, and biliary obstruction.[4–6] Of importance, some of the phase I metabolic genes, such as *Cyp2bs* and *Cyp3as*, which can hydroxylate and facilitate bile acid excretion,[7] are increased during cholestatic liver diseases.[8,9] Consistent with this finding, we observed upregulation of drug metabolic genes specifically in cholestatic mouse livers and not in other liver diseases.

Keywords: Bile acids; Cholestasis; Cytochrome p450; Drug metabolism; Liver diseases; Nuclear receptors; Transcriptomics.
Received 2 December 2019; received in revised form 23 June 2020; accepted 24 June 2020; available online 2 July 2020
* Corresponding author. Address: Department of Molecular and Integrative Physiology, University of Illinois at Urbana-Champaign, Urbana, IL, USA. Tel.: (217) 300-7905, fax: (217) 333-1133.
E-mail address: anakk@illinois.edu (S. Anakk).

As phase I and II genes are transcriptionally regulated by nuclear receptors constitutive androstane receptor (CAR) and pregnane X receptor (PXR),[10] we analysed the liver transcriptome after activating CAR with its ligand and used publicly available PXR data. We hypothesised that increases in CAR activation in the cholestatic double-knockout (DKO) mice might alter drug metabolism. To test this, we examined acetaminophen-induced liver toxicity and zoxazolamine-induced paralysis in control and DKO mice in the presence and absence of CAR inverse agonist, androstanol.

To investigate potential clinical significance, we tested if similar gene expression patterns are maintained in humans by analysing publicly available liver transcriptome data sets of hepatitis B and C viral infections,[11] alcoholic hepatitis (AH),[12] NASH,[13] and biliary atresia.[14] Finally, we evaluated if CYP2B6 protein expression, one of the CAR targets, is altered in biliary atresia patient livers.

Materials and methods

Animals

Fxr$^{-/-}$*Shp*$^{-/-}$ (DKO) male mice were generated as previously described.[15] Age-matched wild-type (WT) males were used as controls. Individual floxed farnesoid X receptor (*Fxr*) and floxed small heterodimer partner (*Shp*) mice obtained from Dr Kristina Schoonjans's laboratory (École Polytechnique Fédérale de Lausanne, Lausanne, Switzerland) were intercrossed to generate double-floxed homozygous *Fxr-Shp* mice (fl/fl *Fxr* fl/fl *Shp*). The mice were housed on a standard 12-h light/dark cycle. All the experiments were carried out on 12- to 16-week-old male mice on C57/B6 background, unless specified, as outlined in the Guide for the Care and Use of Laboratory Animals of the National Academy of Sciences (NIH publication 86-23, revised 1985) and approved by the Institutional Animal Care and Use Committee at University of Illinois at Urbana-Champaign (UIUC; Urbana, IL, USA). To test if increased expression of detoxification genes is a generalised injury response of the liver, the following experimental cohorts were used:

- Bile-acid-induced stress, in which fl/fl *Fxr* fl/fl *Shp* C57/B6 mice were fed with either normal chow or 1% cholic acid (CA) (TD.140532) diet for 5 days
- High-fat-diet-induced fatty liver, in which C57/B6 mice were fed either a chow or 60% fat containing diet (TD.06414) for 8 weeks (this led to steatosis but not NASH)
- Liver regeneration model, in which livers from C3H/HeN mice were collected 48 h post two-thirds PHx to determine if CAR is activated in the regenerating liver

All the mouse diets were obtained from Harlan (ENVIGO, Indianapolis, IN, USA).

Chemicals

Murine CAR agonist 1,4-bis (2-[3,5-dichloropyridyloxy]) benzene (TCPOBOP), referred here as TC, was obtained from Sigma, St. Louis, MO, USA. TC was first dissolved in 100% ethanol at a concentration of 4 mg/ml, followed by dilution in corn oil and stirred overnight to make a final concentration of 2 mg/ml. Thirty-six hours after a single intraperitoneal injection with corn oil or 3 mg/kg TC, WT mice were sacrificed to collect livers. For acetaminophen treatments, WT and DKO mice were fasted overnight, followed by a single intraperitoneal injection with 0.9% saline or 300 mg/kg acetaminophen (Sigma). Another cohort of control and DKO mice were also treated with androstanol (100 mg/kg) 1 h after acetaminophen injection. The mice were then sacrificed to collect liver and blood serum after 1, 6, and 24 h. A 0-h time point was used as controls. WT and DKO mice were injected intraperitoneally once with either 250 mg/kg zoxazolamine (Sigma) alone, or with 100 mg/kg androstanol (Sigma) 3 days before zoxazolamine treatment to inhibit CAR activity. Immediately after zoxazolamine injection, the mice were placed on their backs. The time taken by the mice to regain the righting reflex and start walking was recorded as the paralysis time.

Histology and immuno-staining

Liver tissues were fixed in 10% formalin for 24 h, processed, and embedded in paraffin. Liver sections were cut to obtain 5-μm-thick slices, followed by deparaffinisation in xylene and ethanol (100%, 95%, 80%, and 50%) and rehydration in water. These slices were stained with haematoxylin and eosin as per manufacturer's protocol.

For immunofluorescence staining, the rehydrated sections were antigen retrieved in Tris-EDTA buffer (pH 8.0) in a slow cooker at 90°C for 5 min, followed by cool down in cold tap water. Next, the sections were washed in TBS +0.05% Triton X-100 buffer twice for 5 min, and blocked in 10% normal goat serum and 1% BSA at room temperature for 2 h. Post blocking, anti-CYP2B6 (catalogue number TA504328; OriGene) was applied to the sections at 1:100 dilution and incubated overnight at 4°C. Following this, the sections were washed in TBS + Triton X-100 buffer, and secondary fluorescent antibodies (goat anti-mouse; 1:500 in 1% BSA + TBS) were applied for 1 h at room temperature. The sections were then coverslipped using CC/Mount™ aqueous mounting media (Sigma) and imaged on a ZEISS LSM 710 microscope at the Carl R. Woese Institute for Genomic Biology (IGB) core facility, UIUC. For immunohistochemistry, biliary atresia liver tissue samples were stained with anti-CYP2B6 (catalogue number TA504328; OriGene) at 1:2000 dilution and incubated overnight at 4°C. Following this, the sections were incubated with Vector Immpress anti-mouse ready to use secondary antibody (Vector Biolabs, Burlinghame, CA, USA) and visualized on a Nikon Eclipse Ni microscope at Texas Childrens' Hospital, TX.

RNA-Seq analysis

RNA was isolated using RNeasy Tissue Mini Kit (QIAGEN) from the livers of the following cohorts of mice:

- Cohort 1: chow-fed WT and DKO (*Fxr*$^{-/-}$*Shp*$^{-/-}$ DKO) mice
- Cohort 2: corn oil- or TC-treated WT mice
- Cohort 3: chow- or high-fat-diet-fed WT mice
- Cohort 4: sham or partial hepatectomised (PHx) mice
- Cohort 5: chow- or CA-fed mice

RNA quality was tested using an Agilent bioanalyzer by the Functional Genomics Core at the Roy J. Carver Biotechnology Center, UIUC. Hi-Seq libraries were prepared and Illumina sequencing was performed on a HiSeq 4000 at the High-Throughput Sequencing and Genotyping Unit, UIUC. The sequencing details are outlined in Table S1. Reads were processed for quality using Trimmomatic and aligned to the mouse genome (mm10) using STAR (Spliced Transcripts Alignment to a

Reference). Read count values and differential gene expression were obtained from HTseq and DESeq2, respectively. Fold change >1.5, calculated relative to the respective controls, was considered significant. Log_2 fold change was plotted as heat maps. Up- and downregulated genes were clustered into biological pathways using DAVID Gene Ontology tool (https://david.ncifcrf.gov/tools.jsp).

The data discussed in this publication have been deposited in the NCBI's Gene Expression Omnibus (GEO)[16] and are accessible through GEO series accession number GSE116627 (https://www.ncbi.nlm.nih.gov/geo/query/acc.cgi?acc=GSE116627).

Quantitative Venn diagrams

BioVenn[17] was used to generate Venn diagrams comparing the overlapping phase I and II metabolic genes between the following groups:

- Group 1: DKO, CAR-activated, and PXR-activated mice
- Group 2: DKO, *Fxr*$^{-/-}$ (FXR knockout [FXRKO]), and *Shp*$^{-/-}$ (SHP knockout [SHPKO]) 5-week-old mice[15]
- Group 3: DKO and CA-fed mice

InteractiVenn[18] was used to generate Venn diagrams to depict overlap between human transcriptomic data sets of HBV, HCV, AH, and NASH. Genes showing significant changes were included.

Analysis of serum bile acid composition

Pooled serum from DKO, CA-diet-fed mice, or their respective controls (n = 5 mice per group) was quantitated for individual bile acid species using liquid chromatographic-mass spectrometry at the Metabolomics Core at Baylor College of Medicine, Houston, TX, USA. A Waters ACQUITY UPLC® BEH C18 column was used. L-zeatine was spiked into each sample as an internal standard.

Hepatic glutathione assay

Total hepatic glutathione disulphide (GSH) levels were measured in liver homogenates from WT and DKO mice post acetaminophen treatments using a Glutathione Assay Kit (Sigma-Aldrich, St Louis, MO, USA), according to the manufacturer's protocol. Briefly, total GSH was extracted from liver lysates in 5% sulphosalicylic acid and oxidised to GSSG by 5,5′-dithiobis-(2-nitrobenzoic acid). This is followed by the addition of NADPH to measure the rate of GSH formation in the presence of glutathione reductase kinetically at 412 nm using BioTek Synergy2, Winooski, VT, USA.

Western blotting

Radioimmunoprecipitation assay buffer (25 mM Tris [pH 7], 150 mM NaCl, 0.5% sodium deoxycholate, protease inhibitor [Pierce™ Protease Inhibitor Mini Tablets, EDTA free; Thermo Fisher Scientific], phosphatase inhibitor [Phosphatase Inhibitor Cocktail 3; Sigma-Aldrich], and 1% Triton X-100) was added to each liver sample, which was homogenised, and sonicated to extract proteins. Protein concentration was measured by bicinchoninic acid assay (Pierce BCA Protein Assay Kit; Thermo Fisher Scientific). For Western blot, 50 μg of total protein was loaded onto 8–12% SDS-PAGE gels. After transfer, the membrane was incubated with Cyp2E1 antibody (1:1000; Abcam, Cambridge, MA, USA) followed by goat anti-rabbit secondary antibody (1:5000, GE Healthcare, Chicago, IL, USA). Chemiluminiscence was detected using Bio-rad ChemiDoc system XRS+, Hercules, CA, USA.

qRT-PCR analysis

RNA was isolated from WT and DKO livers (n = 5 per group) using TRIzol™ (Invitrogen), reverse transcribed, and analysed by SYBR® Green™-based qRT-PCR using ABI Quant Studio 3, Thermo Fisher Scientific. Mouse-specific primer sets are listed in Table S2. Relative gene expression was calculated by delta-delta Ct method and normalised to *36b4* levels as loading control.

Statistical analysis

Data are presented as mean ± SEM. Unpaired Student *t* test was used to compare between WT and DKO. One-way ANOVA with a Bonferroni *post hoc* test was used for the zoxazolamine and acetaminophen experiments. Student's *t* test was used for the expression analysis of the human samples. All statistical analyses were done using GraphPad Prism. Correlation was assessed using Pearson correlation coefficient test. Level of significance was $p < 0.05$.

Results

Genome-wide analysis of diseased murine and human livers revealed upregulation of drug metabolic genes during cholestasis

The liver is a central hub responsible for the breakdown of carbohydrates, fat, protein, and foreign compounds, including prescription drugs. To examine the alterations in transcriptional programmes during different insults to the liver, we performed and analysed RNA-seq on cholestatic, fatty, and regenerating mouse livers. As a model of cholestatic liver disease, we employed the combined deletion of both *Fxr* and *Shp* (DKO), which accumulate excessive bile acids.[15,19] Histological analysis revealed hepatocyte ballooning, ductular reactions, and focal inflammation, consistent with severe cholestasis in the DKO livers. Mice fed with high-fat diet, as expected, developed macrosteatosis and fatty liver, and PHx resulted in a robust regenerative response, indicated by the presence of mitotic bodies (Fig. S1).

During cholestasis, many metabolic pathways, including drug metabolism, were upregulated, whereas DNA damage, hypoxia, and insulin response were downregulated (Fig. 1A). As expected, the livers of mice fed with high-fat diet showed upregulation of genes related to lipid transport, immune response activation, and acyl CoA metabolism, whereas regenerating livers showed upregulation of genes related to cell cycle, mitosis, and acute phase response. Interestingly, both models exhibited downregulation of glucose homeostasis, oxidation-reduction, steroid, and P450-dependent metabolic pathways (Fig. 1B and C). When we assessed common pathways between the three mouse models, gene ontology analysis revealed enrichment in cellular proliferation, inflammation, and downregulation of glucose and lipid homeostasis (Fig. 1D; Table S3).

As many liver disorders exhibit accumulation of bile acids, we examined the cholestatic DKO mice and found a specific increase in the P450 metabolic gene profile. This led us to focus on drug metabolism. To test if bile acid overload can activate drug-metabolising phase I and II genes, we examined the liver transcriptomes of CA-fed WT and DKO mice. Both groups revealed the upregulation of oxidation-reduction, glutathione metabolism,

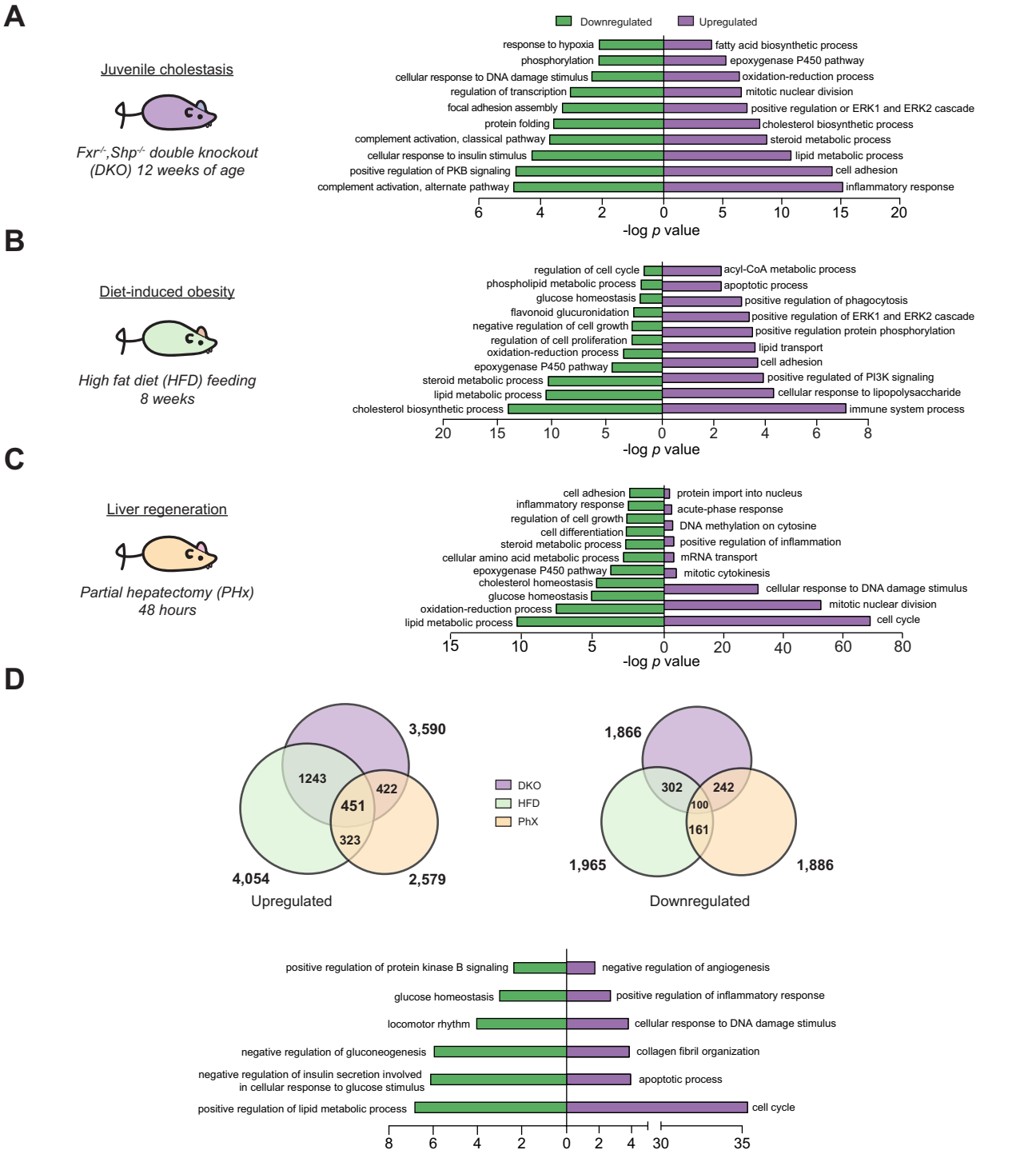

Fig. 1. Genome-wide profiling reveals common and unique gene networks in cholestasis, steatosis, and regeneration. Specific up- and downregulated pathways in (A) cholestatic (double knockout [DKO]), (B) diet-induced steatosis (high-fat diet [HFD]), and (C) regenerating (partial hepatectomy [PHx]) livers are shown. (D) Venn diagrams represent the overlap of either downregulated or upregulated gene expression amongst mouse models of cholestasis, fatty, and regeneration. Bar graph exhibits DAVID Gene Ontology network analysis for the common pathways in these diseased models. (n = 2–3 mice per group; fold change >1.5; FDR <30).

and cellular drug response pathways with a 95% overlap in phase I and II metabolic gene expression (Fig. S2A–C; Fig. 1A). As expected, these two mouse models exhibited increased total serum bile acids and changes in bile acid composition[15,20] with CA levels increased upon CA diet. By contrast, T-CA and T-MCA were high in DKO mice (Fig. S2D–F).

Transcriptome profile of cholestatic DKO livers overlaps mainly with CAR activation

Nuclear receptors CAR and PXR coordinate phase I and II metabolic genes to detoxify and clear foreign compounds.[21,22] Therefore, we performed RNA-seq analysis of livers after activation of CAR (TC treated), and compared it with the DKO data

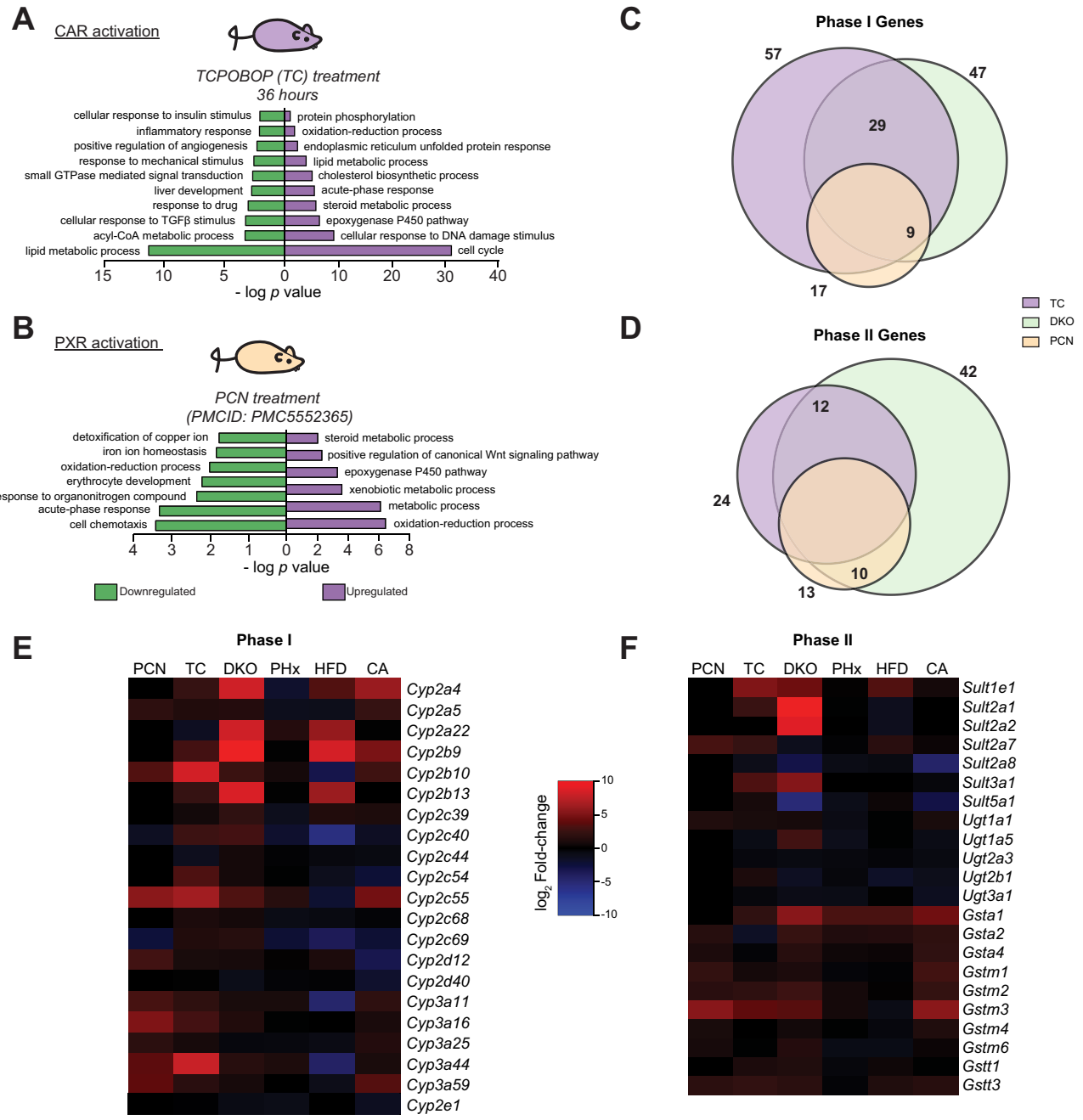

Fig. 2. Constitutive androstane receptor (CAR) target signatures are induced specifically in cholestatic conditions. Bar graphs show upregulated and downregulated biological pathways in (A) CAR- and (B) pregnane X receptor (PXR)-activated livers (n = 2–3 mice per group; Unpaired Student's *t* test; fold change >1.5; FDR <30). Venn diagrams show major overlap of (C) phase I genes between 1,4-bis (2-[3,5-dichloropyridyloxy]) benzene (TC)-treated and double-knockout (DKO) mice. (D) Phase II genes in DKO livers are equally spaced between TC- and pregnenolone 16 alpha-carbonitrile (PCN)-treated mice. Numbers indicate total number of genes in individual conditions and overlap of DKO with TC and PCN (n = 3 per group; Unpaired Student's *t* test; fold change >1.5; p <0.05). Heat maps represent that the cholestatic DKO livers recapitulate profiles of (E) phase I and (F) phase II genes observed in TC-treated (CAR-activated) livers (n = 2–3 mice per group; Unpaired Student's *t* test; fold change >1.5, p <0.05). Importantly, some of these gene changes were mimicked in bile acid (cholic acid) diet, but not in PCN-treated (PXR activated), high-fat diet (HFD), and partial hepatectomy (PHx) livers.

and the published PXR-activated (pregnenolone 16 alpha-carbonitrile [PCN]-treated) data set.[23] TC and PCN treatments caused the upregulation of xenobiotic and steroid metabolism (Fig. 2A and B) with the expected *Cyp2bs* and *2cs* response in CAR and *Cyp3as* response in PXR. We also found a strong upregulation of cell-cycle-associated transcripts with TC treatment, suggesting an essential role for CAR in proliferation. Further, the changes in DKO livers showed approximately 37% (Fig. S3A) overlap with the entire CAR-activated genes. When we narrowed on drug-metabolising genes, DKO expression profile overlapped 46% (41/89 genes) with CAR activation *vs.* 21% (19/89) with PXR-activated genes (Fig. 2C and D).

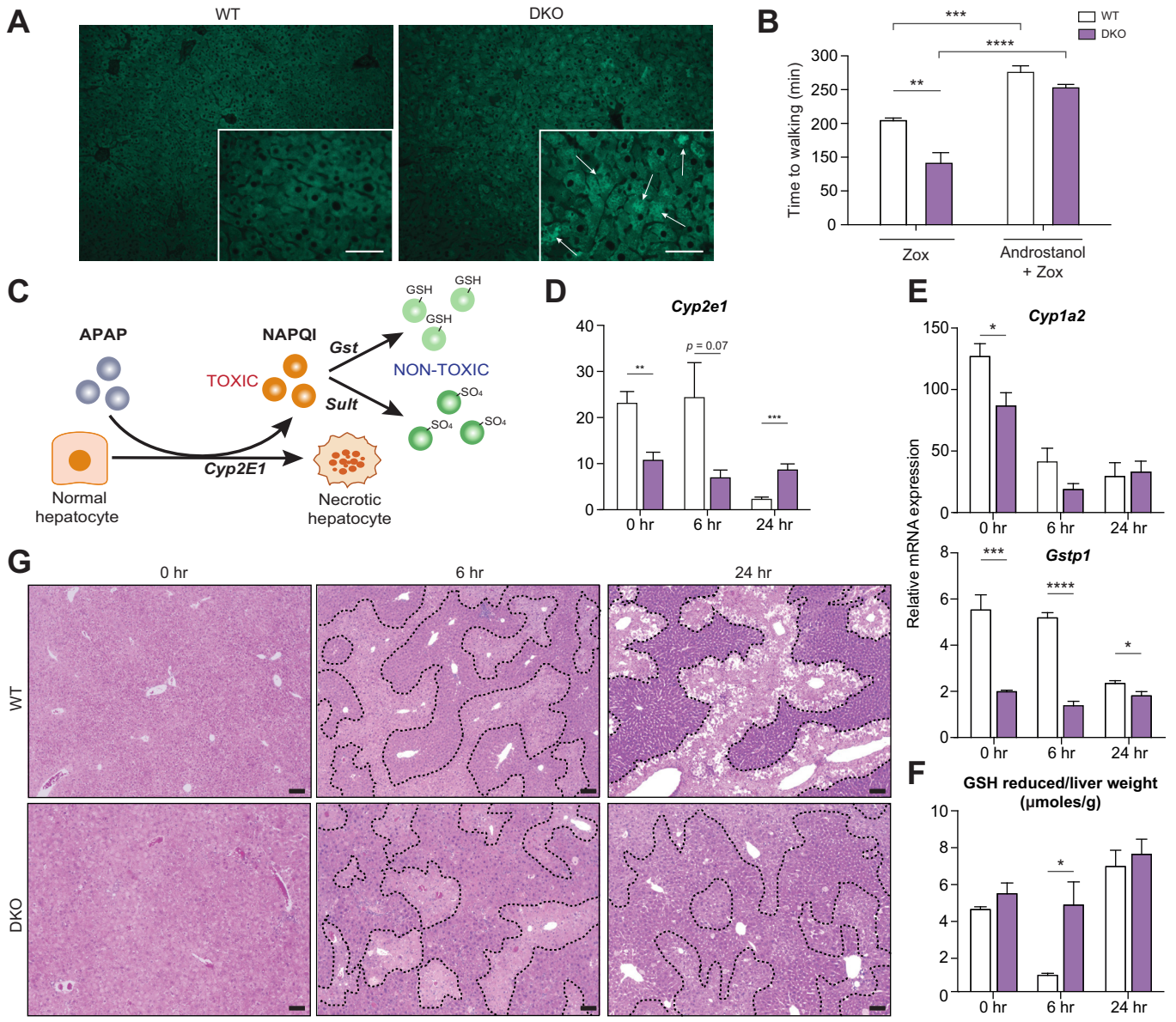

Fig. 3. Changes in phase I and II genes in cholestatic mice result in protection against zoxazolamine and acetaminophen (APAP) toxicity. (A) Double-knockout (DKO) cholestatic livers show increased immunofluorescence staining for CYP2B6 compared with wild-type (WT) livers (n = 4–5 mice per group; scale bar: 50 μm). (B) Bar graph indicates that DKO mice recover faster post zoxazolamine (zox)-induced paralysis than WT mice. Inhibiting constitutive androstane receptor activity with androstanol normalises the difference in paralysis time between WT and DKO mice (n = 3–4 mice per group; mean ± SEM; one-way ANOVA; $^{**}p$ <0.01). (C) Schematic of acetaminophen metabolism in the liver. (D and E) qPCR analysis shows upregulation of key genes involved in APAP metabolism in DKO livers (n = 4–6 mice per group; Student's *t* test; $^{*}p$ <0.05). (F) Hepatic glutathione disulphide (GSH) levels at different time points post-APAP treatment in control WT and cholestatic DKO mice. (G) Histological analysis of liver sections at 0, 6, and 24 h after APAP injection shows reduced necrosis in the DKO compared with WT mice (n = 4–6 mice per group; mean ± SEM; one-way ANOVA; $^{*}p$ <0.05, $^{**}p$ <0.01, $^{***}p$ <0.005, $^{****}p$ <0.001).

CA-fed livers mimicked the profile of cholestatic DKO mice with increases in phase I genes. However, 48 h after PHx, and in diet-induced steatosis, *Cyp450* genes remained suppressed (Fig. 2E). Phase II sulphotransferase (*Sult*) genes were robustly induced only in DKO and TC-treated WT mice. By contrast, increases in glutathione sulphotransferases (*Gsts*) were observed in DKO, CA-fed, and PCN- and TC-treated mice, but not in the steatotic and regenerating livers, except *Gsta1* (Fig. 2F).

As the cholestatic DKO mice exhibited increases in drug metabolism genes, we investigated if this is a consequence of *Fxr* and *Shp* deletion. We compared DKO, FXRKO, and SHPKO livers, and found that *CYP450* drug metabolism genes were unaltered except for increased expression of *Cyp2a5* and *Cyp2c39* in FXRKO (Fig. S3B and C). By contrast, the expression of several *Gst* genes was higher in both DKO and FXRKO, but their levels were reduced in SHPKO livers (Fig. S3D and E).

CAR is responsible for increased phase I gene expression in cholestasis

CYP2Bs and CYP3As orchestrate phase I metabolism of many of the commonly prescribed drugs and are regulated by CAR activity[24] (Table S4). qRT-PCR validated our RNA-seq results, such that *CYP450* genes, including *Cyp2b10* and *Cyp3a11*, were induced along with alterations in *Sults* and *Gsts* in the cholestatic DKO mice (Fig. 2; Fig. S4A). We further examined the protein expression of CYP2B6, a CAR target protein, and found it elevated in the DKO livers (Fig. 3A). To test the functional consequence of this expression profile, we used a pharmacological approach. We treated WT and DKO mice with the paralytic agent zoxazolamine and found that DKOs exhibited lower paralysis time compared with WT mice (Fig. 3B). Inhibiting CAR activity with androstanol was sufficient to increase paralysis time both in WT and DKO (Fig. 3B). To test the consequence of CAR activation on a commonly used prescription drug, we challenged WT and DKO mice with high doses of acetaminophen (APAP), which causes severe hepatotoxicity (Fig. 3C).

Despite serum ALT and AST being higher at baseline as well as 1 h post APAP, the fold change of this increase at 6- and 24-h time point is lower in the DKO compared with control mice (Fig. 4A; Fig. S4B). We examined transcript expression of *Cyp2e1*, which is responsible for converting APAP to the toxic *N*-acetyl-*p*-benzoquinone imine (NAPQI) metabolite, and found it to be lower at baseline but was higher at the 24-h time point in the DKO mice (Fig. 3D). Further, cholestatic mice showed a decrease in *Cyp1a2* and *Gstp1* (Fig. 3E), which correlated well with a higher concentration of reduced GSH at the 6-h time point (Fig. 3F) and protection against liver injury (Fig. 3G). To investigate the early response to APAP toxicity, we analysed reduced GSH levels, and they plummeted 1 h post-injection in both WT and DKO mice. No difference in CYP2E1 protein expression was observed, suggesting that the initial injury is similar between the two groups (Fig. 4A–F). We postulated that CAR-mediated phase I and II genes protected the DKO mice, and to test this, we challenged mice with APAP and inhibited CAR activity using androstanol. Serum liver injury markers, ALT, and AST were elevated to the same extent as control, and reduced GSH levels were significantly lowered in DKO mice upon androstanol treatment (Fig. 4G–L). These experiments highlight the relevance of CAR activation in protecting the DKO mice from APAP toxicity and zoxazolamine-induced paralysis.

Drug-metabolising genes are induced in biliary atresia patients

To determine if phase I drug metabolism is induced in human liver diseases, we first analysed the liver transcriptomes of post-HBV or -HCV infected,[11] AH,[12] NASH,[13] and biliary atresia[14] patient cohorts. We did not find significant overlap in gene expression between these different human cohorts (Fig. 5A). Interestingly, gene ontology pathway analysis revealed upregulation of P450 pathway in biliary atresia transcriptome (Fig. 5B; Fig. S5). Although the gene ontology 'response to drugs' was upregulated in viral infections (Fig. S5A), this was not related to the P450 detoxification genes. However, we found a robust decrease in *CYP2C19* and *UGT2A1* in post-HCV group (Fig. 5C and D). Additionally, transcriptomic data analysis from patient samples with AH[12] revealed an overall downregulation of phase I and II genes, except for *CYP1B1* and *SULT1C2* expression. Similarly, NASH liver samples[13] also exhibited reduced expression of many phase I genes except for induction in *CYP3A5*, *CYP3A7*, and *CYP3A43* along with *SULT1C2* and *UGT2B28* (Fig. 5C and D).

Moreover, we mined publicly available biliary atresia transcriptomic data for the expression profile of detoxification genes.[14,25] Biliary atresia samples compared with normal control sample displayed increases in *CYP3A7* and several *SULT* and *UGT* detoxification genes (Fig. 5C and D). Further, we found dramatically high coefficient of variation 70–150% within samples: normal controls (n = 7) and biliary atresia (n = 161). We compared within the biliary atresia (22–169 days old) samples rather than comparing with control deceased liver samples (1.8–3.5 years old) because *CYP* expression changes markedly with age.[26] We segregated the biliary atresia sample based on serum gamma-glutamyl transferase (GGT) levels. In this manner, we were able to identify samples with dramatically elevated GGT, which correlate with higher expression of drug metabolism genes. We found that the phase I and II gene expression pattern segregated into three categories (Figs. 5 and 6) based on GGT levels: low (<450 U/L; n = 21), mid (450–850 U/L; n = 31), or high (>850 U/L; n = 17). Notably, 25% of the samples fell within the high-GGT category, and this displayed induction of several phase I genes, including *CYP2C8* and *CYP3A4* (Figs. 5C and 6A). *CYP2B6* transcript expression, however, did not reach statistical significance as a result of a high coefficient of variation (97.40%). The gene expression pattern of the mid-GGT group revealed a similar trend to that of high GGT (Fig. S6A). Most of the phase II genes remained unaltered in biliary atresia except for reductions in *SULT1E1* and *UGT3A1* expression (Figs. 5D and 6B; Fig. S6B). CAR and PXR activation is known to suppress these two phase II genes,[27–29] indicating that the xeno-sensing mechanism may be active in patients with high GGT.

Finally, we stained the biliary atresia patient samples for hepatic CYP2B6 protein expression and found this CAR target significantly elevated to different degrees in them (Fig. 6C; Fig. S7). The variation in increased CYP2B6 expression did not correlate with the serum liver injury markers (Table S5). Nevertheless, these clinical samples corroborate our results from the DKO and CA-fed mouse models, and implicate that activation of CAR in cholestasis can lead to alterations in drug metabolism with beneficial effects against hepatotoxicity (graphical abstract).

Discussion

In this study, we took a genome-wide approach to investigate pathways that are altered under different conditions of liver diseases using mouse models and by mining publicly available human data. Analysis of common and distinct molecular pathways revealed an increase in cytochrome P450 genes particularly during cholestasis. We focused on cytochrome P450s because they are fundamentally responsible for drug metabolism, and therefore, for therapeutic outcomes.

Also, xeno-sensors CAR and PXR transcriptionally regulate drug metabolism; therefore, we compared RNA-seq data from different liver injury models with either activation of CAR or PXR.[23,30] This analysis revealed a substantial overlap of gene profiles of cholestasis with CAR activation. As DKO mouse model is a genetic loss of FXR and SHP, we examined and found that the activation of CAR and PXR is not a default consequence of the deletion. We did observe one of the drug-metabolising genes, *Cyp2c8*, correlates with *Fxr* expression (Fig. S6C). We postulate this could be secondary to hepatocyte nuclear factor 4 alpha (Hnf4α), which is known to mediate *Cyp2c8* regulation.[31]

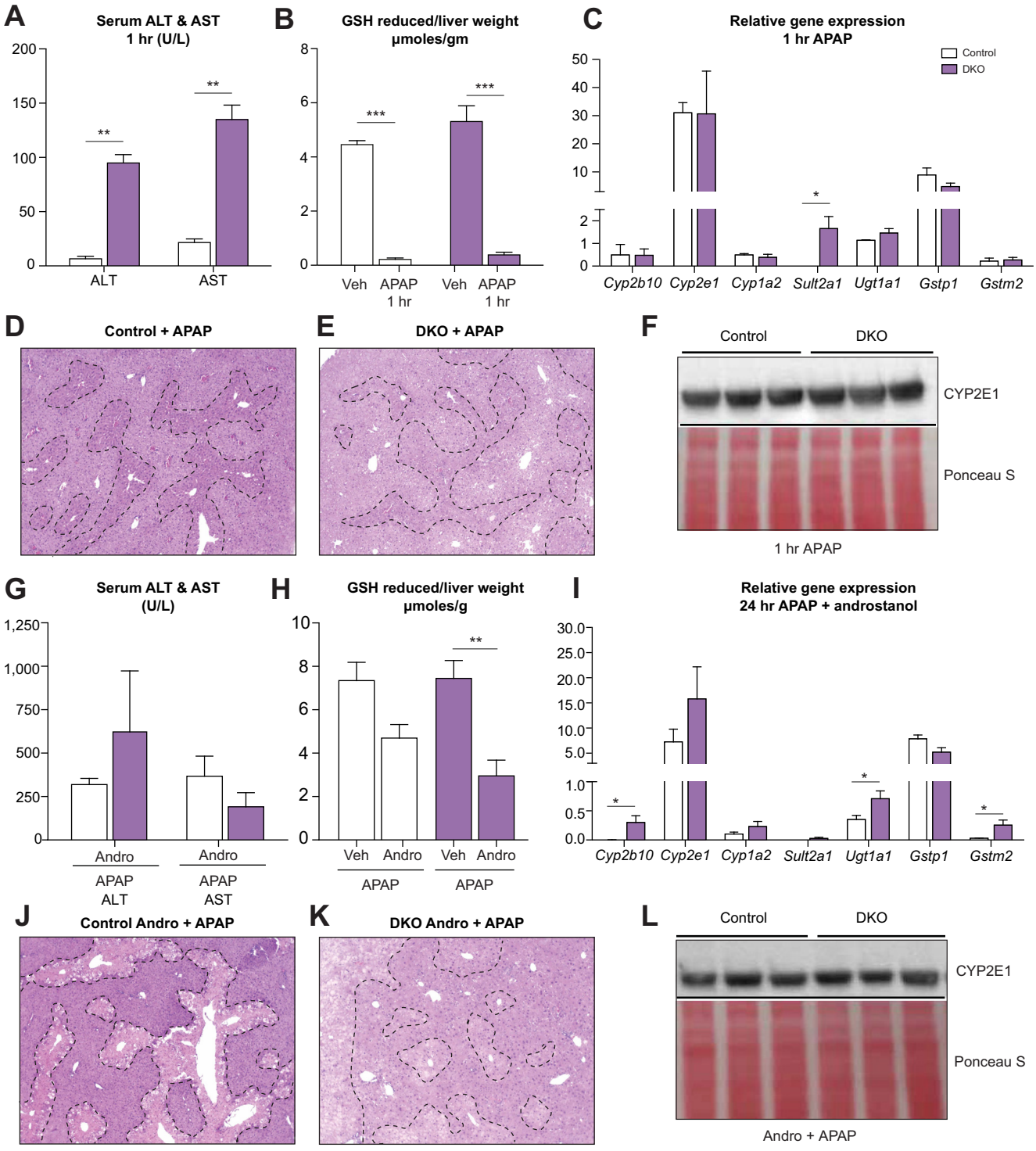

Fig. 4. Inhibition of constitutive androstane receptor (CAR) activity makes double-knockout (DKO) cholestatic livers susceptible to acetaminophen (APAP)-mediated toxicity. Bar graphs show (A) serum liver injury markers and (B) hepatic glutathione disulphide (GSH) levels 1 h post-APAP treatment in control wild-type (WT) and cholestatic DKO mice. (C) qPCR analysis depicts no difference in the expression of key genes involved in phase I and II detoxification. (D and E) Histological analysis at 1 h after APAP injection shows similar necrosis in both the DKO and WT liver sections. (F) Post 1 h of APAP injection; no change in CYP2E1 protein levels is observed (n = 3 mice per group; Student *t* test; $^{*}p$ <0.05). Bar graphs show (G) no significant difference in serum liver injury markers, but (H) lower hepatic GSH levels in DKO mice injected with androstanol, a CAR antagonist, 1 h post-APAP treatment. (I) qPCR analysis depicts an upward trend in the expression of key genes involved in phase I and II detoxification in DKO mice. (J and K) Histological analysis revealed significant necrosis in DKO livers injected with androstanol compared with those in Fig. 3. However, the injury is still less severe than WT liver sections. (L) No difference in CYP2E1 protein levels is observed (n = 5 mice per group; one way ANOVA; $^{*}p$ <0.05, $^{**}p$ <0.005, $^{***}p$ <0.0005).

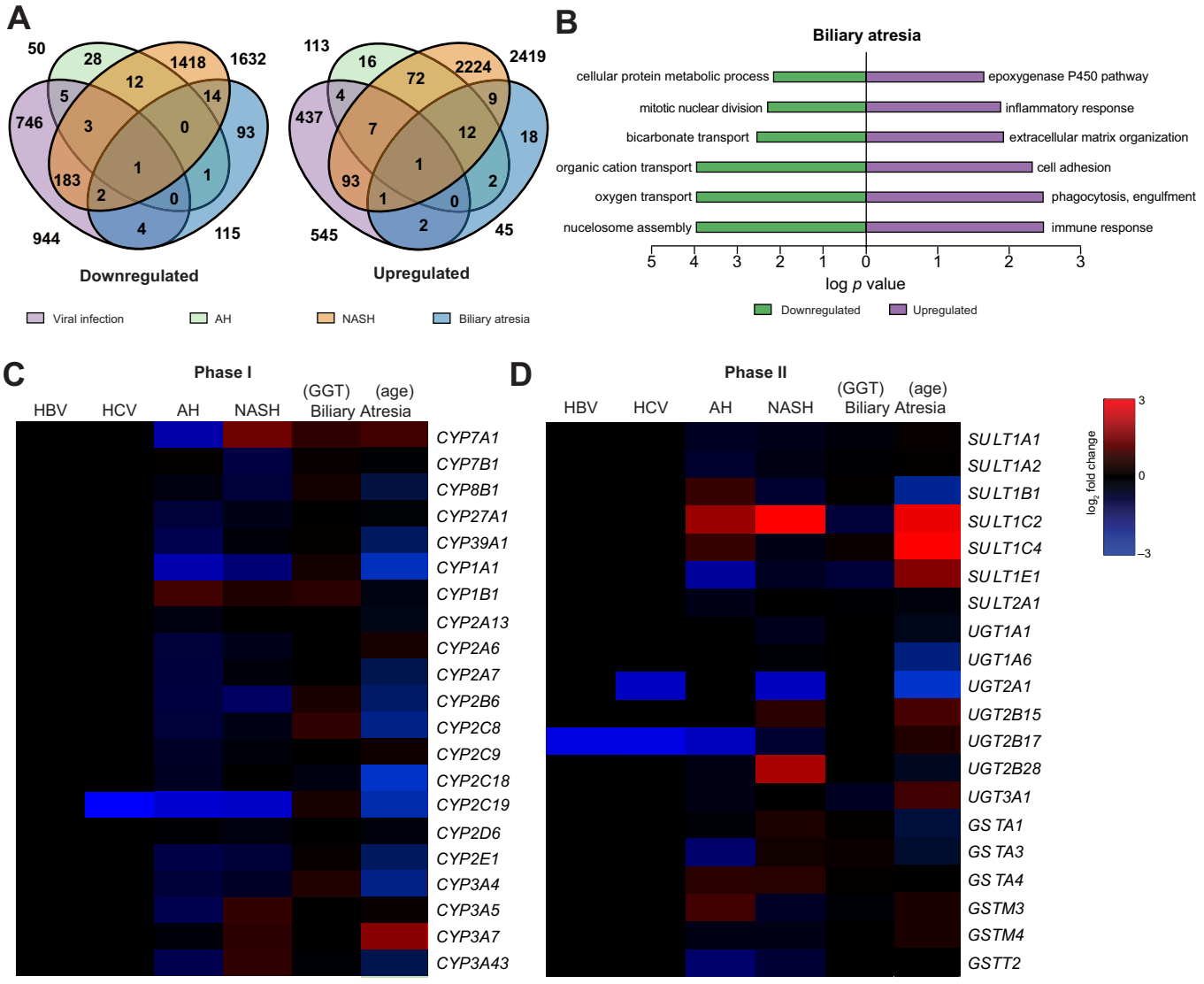

Fig. 5. Comparative transcriptomic analyses indicate that drug metabolism is not a generalised response to liver injury. Previously conducted transcriptomic data analyses for liver injury models in patient samples with viral (both hepatitis B and C) infection, alcoholic hepatitis (AH) (Gene Expression Omnibus [GEO] data set: GSE28619), non-alcoholic steatohepatitis (NASH) (GEO data set: GSE126848), and biliary atresia (GEO data sets: GSE46995 and GSE122340) were mined for alterations in gene expression. (A) Venn diagrams show little overlap in gene expression amongst these liver diseases. (B) Bar graph shows upregulated and downregulated biological pathways in livers from biliary atresia patients (Unpaired Student's *t* test; fold change >1.5; FDR <30). Heat maps display (C) phase I and (D) phase II drug metabolic genes in the liver diseases (Unpaired Student's *t* test; fold change >1.5; p <0.05). Biliary atresia gene expression profile was separated either by circulating gamma-glutamyl transferase (GGT) levels or by age.

Moreover, FXRKO, SHPKO, and *Bsep*KO (deletion of bile salt canalicular exporter *Bsep*) do not accumulate bile acids to the extent of DKO or 1% CA-diet-fed mice,[19,20] and did not exhibit activation in phase I genes. These data suggest that a particularly high threshold of bile acid concentration is necessary to promote activation of detoxification pathways in the liver.

We tested the functionality of these changes in mice by measuring APAP toxicity and the zoxazolamine paralysis effect. CAR activation is associated with increased sensitivity to APAP toxicity.[32] Surprisingly, DKO mice showed resistance to APAP toxicity. On examining further, in line with CAR activation, we did observe reduced basal expression of *Cyp2e1*, which is important for metabolising APAP and NAPQI generation. However, we did not find any difference in *Cyp2e1* mRNA and protein expression 1 h after APAP. In fact, *Cyp2e1* expression was induced at the 24-h time point after APAP injection in DKO livers. This result indicated that the protection from APAP toxicity could be attributable to the phase II response. Therefore, we analysed the expression of different glutathione S-transferase genes and found *Gstp1* expression was reduced. Consistently, we found that glutathione levels plunged at 1 h, but rebound and stably maintained in the DKO mice. Inhibiting CAR activity was enough to decrease significant protection to APAP toxicity in the DKO mice. Furthermore, even control animals exhibited a decrease in the concentrations of reduced GSH, albeit not reaching significance after androstanol treatment. Recently, bile acids, as well as *Gstp1/2* deletion, were shown to cause resistance to APAP toxicity.[33–36] Thus, bile acids and CAR-driven mechanisms may

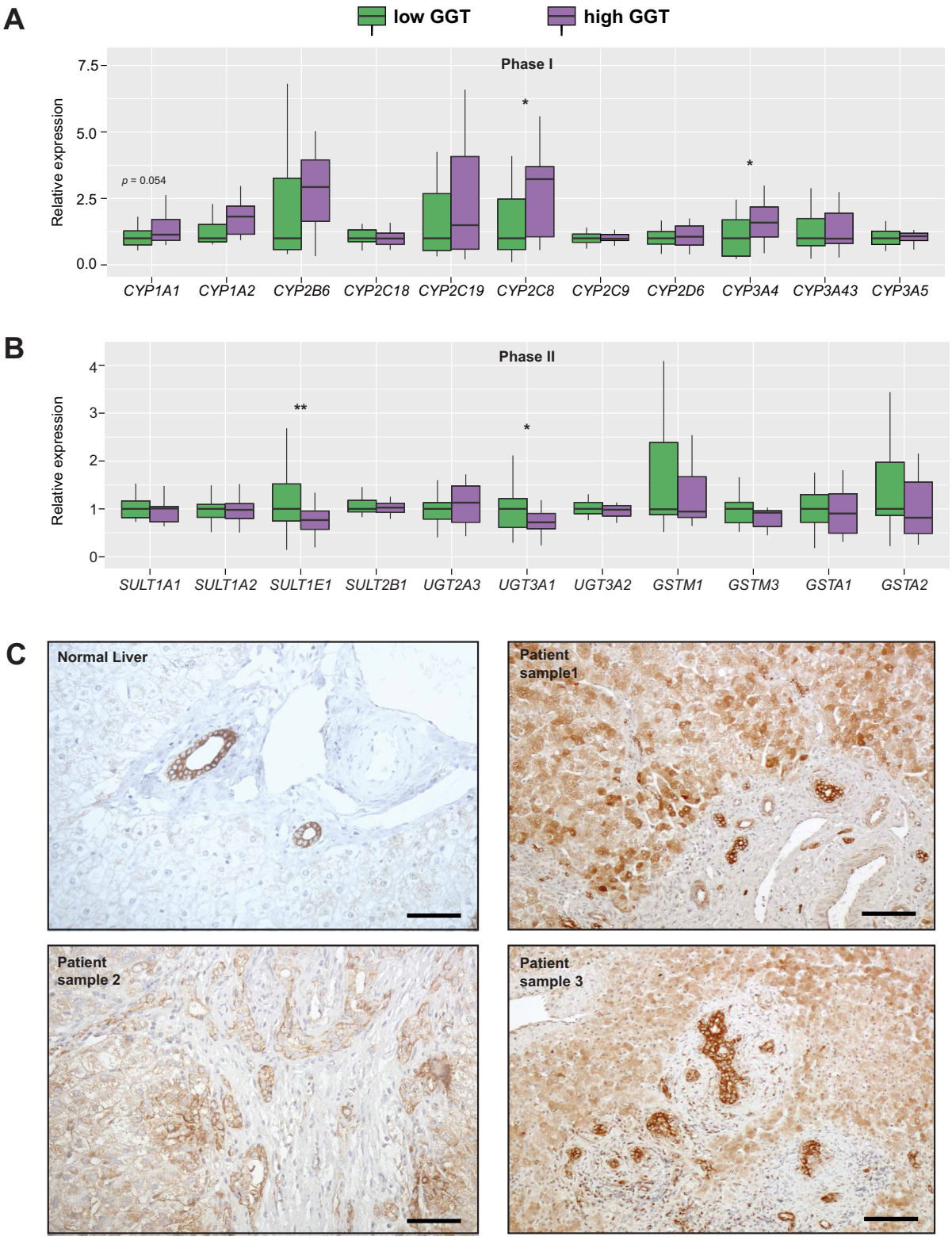

Fig. 6. Biliary atresia patients demonstrate increased activation of constitutive androstane receptor downstream targets. Based on drug metabolic gene expression, microarray data for biliary atresia (Gene Expression Omnibus data set: GSE46995) were segregated into two groups: low gamma-glutamyl transferase (GGT) <450 IU/L (n = 21) and high GGT >850 IU/L (n = 17). Box plots show relative expression for (A) phase I and (B) phase II genes. mRNA expression was normalised to the median value of the low-GGT group (Student *t* test; **p* <0.05, ***p* <0.01). (C) Immunohistochemical staining of CYP2B6 reveals robust staining in biliary epithelial cells, nerves, and in hepatocytes with an overall increase in its expression in biliary atresia samples compared with control.

protect the DKO mice from APAP toxicity. Similarly, androstanol treatment increased the zoxazolamine-induced paralysis time in DKO animals, thus underscoring the relevance of CAR activation and pharmacological effects of drugs in cholestasis.

To explore the clinical significance of our findings, we mined the available data sets for different liver disease states caused by HBV or HCV infection, AH, NASH, and biliary atresia. We did not find increases in expression of drug metabolism genes in any of these liver disease conditions except in biliary atresia samples with GGT levels >850 U/L. We do not know why such a significant correlation exists in this high-GGT group, which accounts for 25% of these patients. All biliary atresia patients displayed elevated conjugated bilirubin levels to the same extent (~5 mg/dl) and, unlike serum GGTs, did not separate into distinct clusters. FXR and SHP expression is reduced in biliary atresia, and we examined if there was a correlation between these receptors and CAR, PXR, and P450 genes in humans (Fig. S6). Except for a direct correlation of FXR expression with CYP2C8 and CYP3A4, and SHP with CAR, we found no other statistically significant associations.

Humans have fewer P450s compared with mice; however, nuclear receptors CAR and PXR are known to regulate drug metabolism in both species.[30,37,38] We examined and validated higher expression of CYP2B6 protein, key CAR target, in biliary atresia patient samples. Several studies in the 1970s reported faster clearance of drugs in patients with liver disease. For instance, tolbutamide was metabolised faster in cholestatic patients (165 ± 48 min) compared with normal individuals (384 ± 76 min).[39] Patients with chronic alcohol consumption also had higher metabolism of antipyrine (11.7 *vs.* 15.7 h), phenobarbital (26.3 *vs.* 35.1 h), and warfarin (26.5 *vs.* 41.1 h).[9] Many of these drugs are prototypical substrates of the CAR/PXR target genes *CYP2C*, *2B*, or *3A*.

Although we see higher phase I gene and protein expression, validation of P450 activity in different human cholestatic conditions is challenging.

In summary, we suggest that severely cholestatic human hepatocytes may mount a detoxification response to lower its BA burden. In line with our findings, recent clinical data of 171 biliary atresia patients revealed enrichment in phase I, phase II, and glutathione metabolic pathways in the subset of high-survival patients.[25] Further, lower therapeutic benefits of certain prescription drugs (tolbutamide, warfarin, antipyrine, and phenytoin)[9,39] have been previously reported in individuals with cholestasis. Our findings not only explain this variability, which could be subsequent to CAR activation, but also reveal that modulating CAR may improve clinical outcomes in the management of cholestatic diseases.

Abbreviations

AH, alcoholic hepatitis; ALT, alanine aminotransferase; APAP, acetaminophen; AST, aspartate aminotransferase; CA, cholic acid; CAR, constitutive androstane receptor; DKO, double knockout; *Fxr*, farnesoid X receptor; FXRKO, FXR knockout; GGT, gamma-glutamyl transferase; GSH, glutathione disulphide; NAPQI, *N*-acetyl-*p*-benzoquinone imine; NASH, non-alcoholic steatohepatitis; PCN, pregnenolone 16 alpha-carbonitrile; PHx, partial hepatectomy; PXR, pregnane X receptor; *Shp*, small heterodimer partner; SHPKO, SHP knockout; WT, wild type.

Financial support

This work was supported by the National Institutes of Health/National Institute of Diabetes and Digestive and Kidney Diseases (R01 DK113080), American Cancer Society Research Scholar Grant (ACS 132640-RSG) and start-up funds from the University of Illinois at Urbana-Champaign to SA.

Conflict of interest

The authors declare no conflicts of interest that pertain to this work.

Please refer to the accompanying ICMJE disclosure forms for further details.

Authors' contributions

BM, WA, and MEP did the experiments and data analysis. BM, WA, MEP, AK, SH, and SA did the interpretation of data. BM and SA wrote the article. KS shared the individual *f/fShp* and *f/f Fxr* mice. RF and AMW were responsible for partial hepatectomy and regeneration studies. BM, RF, and WA performed and analysed RNA sequencing. MEP and SA performed the zoxazolamine experiment. JL and SA performed the acetaminophen toxicity experiment. MEP with input from SA put together the drug table. JY and SH performed immunostaining in biliary atresia samples. BM and WA analysed the publicly available transcriptome data. SA was responsible for the study design, editing the article, and study supervision.

Supplementary data

Supplementary data to this article can be found online at https://doi.org/10.1016/j.jhepr.2020.100140.

References

Author names in bold designate shared co-first authorship

[1] Zollner G, Trauner M. Mechanisms of cholestasis. Clin Liver Dis 2008;12:1–26.
[2] Srivastava A. Progressive familial intrahepatic cholestasis. J Clin Exp Hepatol 2014;4:25–36.
[3] Hofmann AF. Bile acids: trying to understand their chemistry and biology with the hope of helping patients. Hepatology 2009;49:1403–1418.
[4] Iqbal S, Vickers C, Elias E. Drug metabolism in end-stage liver disease. In vitro activities of some phase I and phase II enzymes. J Hepatol 1990;11:37–42.
[5] Elbekai RH, Korashy HM, El-Kadi AOS. The effect of liver cirrhosis on the regulation and expression of drug metabolizing enzymes. Curr Drug Metab 2004;5:157–167.
[6] Chai J, Feng X, Zhang L, Chen S, Cheng Y, He X, et al. Hepatic expression of detoxification enzymes is decreased in human obstructive cholestasis due to gallstone biliary obstruction. PLoS One 2015;10:e0120055.
[7] Li T, Chiang JYL. Nuclear receptors in bile acid metabolism. Drug Metab Rev 2013;45:145–155.
[8] Carulli N, Manenti F, Gallo M, Salvioli GF. Alcohol-drugs interaction in man: alcohol and tolbutamide. Eur J Clin Invest 1971;1:421–424.
[9] Hoyumpa AM, Schenker S. Major drug interactions: effect of liver disease, alcohol, and malnutrition. Annu Rev Med 1982;33:113–149.
[10] Willson TM, Kliewer SA. PXR, CAR and drug metabolism. Nat Rev Drug Discov 2002;1:259–266.
[11] Selitsky SR, Dinh TA, Toth CL, Kurtz CL, Honda M, Struck BR, et al. Transcriptomic analysis of chronic hepatitis B and C and liver cancer reveals microRNA-mediated control of cholesterol synthesis programs. mBio 2015;6:e01500–e01515.
[12] Affò S, Dominguez M, Lozano JJ, Sancho-Bru P, Rodrigo-Torres D, Morales-Ibanez O, et al. Transcriptome analysis identifies TNF superfamily receptors as potential therapeutic targets in alcoholic hepatitis. Gut 2013;62:452–460.
[13] **Suppli MP**, **Rigbolt KTG**, Veidal SS, Heebøll S, Eriksen PL, Demant M, et al. Hepatic transcriptome signatures in patients with varying degrees of nonalcoholic fatty liver disease compared with healthy normal-weight individuals. Am J Physiol Gastrointest Liver Physiol 2019;316:G462–G472.

[14] **Bessho K**, **Mourya R**, Shivakumar P, Walters S, Magee JC, Rao M, et al. Gene expression signature for biliary atresia and a role for interleukin-8 in pathogenesis of experimental disease. Hepatology 2014;60:211–223.
[15] Anakk S, Watanabe M, Ochsner SA, McKenna NJ, Finegold MJ, Moore DD. Combined deletion of Fxr and Shp in mice induces Cyp17a1 and results in juvenile onset cholestasis. J Clin Invest 2011;121:86–95.
[16] Edgar R. Gene expression omnibus: NCBI gene expression and hybridization array data repository. Nucleic Acids Res 2002;30:207–210.
[17] Hulsen T, de Vlieg J, Alkema W. BioVenn—a web application for the comparison and visualization of biological lists using area-proportional Venn diagrams. BMC Genomics 2008;9:488.
[18] Heberle H, Meirelles VG, da Silva FR, Telles GP, Minghim R. InteractiVenn: a web-based tool for the analysis of sets through Venn diagrams. BMC Bioinformatics 2015;16:169.
[19] Kim KH, Choi JM, Li F, Arizpe A, Wooton-Kee CR, Anakk S, et al. Xenobiotic nuclear receptor signaling determines molecular pathogenesis of progressive familial intrahepatic cholestasis. Endocrinology 2018;159:2435–2446.
[20] Song P, Zhang Y, Klaassen CD. Dose-response of five bile acids on serum and liver bile acid concentrations and hepatotoxicity in mice. Toxicol Sci 2011;123:359–367.
[21] Xie W, Barwick JL, Simon CM, Pierce AM, Safe S, Blumberg B, et al. Reciprocal activation of xenobiotic response genes by nuclear receptors SXR/PXR and CAR. Genes Dev 2000;14:3014–3023.
[22] Wei P, Zhang J, Dowhan DH, Han Y, Moore DD. Specific and overlapping functions of the nuclear hormone receptors CAR and PXR in xenobiotic response. Pharmacogenomics J 2002;2:117–126.
[23] Cui JY, Klaassen CD. RNA-Seq reveals common and unique PXR- and CAR-target gene signatures in the mouse liver transcriptome. Biochim Biophys Acta 2016;1859:1198–1217.
[24] Wrighton S, VandenBranden M, Ring B. The human drug metabolizing cytochromes P450. J Pharmacokinet Pharmacodyn 1996;24:461–473.
[25] **Luo Z**, **Shivakumar P**, Mourya R, Gutta S, Bezerra JA. Gene expression signatures associated with survival times of pediatric patients with biliary atresia identify potential therapeutic agents. Gastroenterology 2019;157:1138–1152.e14.
[26] Nebert DW, Gonzalez FJ. P450 genes: structure, evolution, and regulation. Annu Rev Biochem 1987;56:945–993.
[27] Li CY, Cheng SL, Bammler TK, Cui JY. Neonatal activation of the xenobiotic-sensors PXR and CAR results in acute and persistent down-regulation of PPARα-signaling in mouse liver. Toxicol Sci 2016;153:282–302.
[28] Lambert CB, Spire C, Claude N, Guillouzo A. Dose- and time-dependent effects of phenobarbital on gene expression profiling in human hepatoma HepaRG cells. Toxicol Appl Pharmacol 2009;234:345–360.
[29] Kodama S, Hosseinpour F, Goldstein JA, Negishi M. Liganded pregnane X receptor represses the human sulfotransferase SULT1E1 promoter through disrupting its chromatin structure. Nucleic Acids Res 2011;39:8392–8403.
[30] Cheng SL, Bammler TK, Cui JY. RNA sequencing reveals age and species differences of constitutive androstane receptor-targeted drug-processing genes in the livers. Drug Metab Dispos 2017;45:867–882.
[31] Hwang-Verslues WW, Sladek FM. HNF4α-role in drug metabolism and potential drug target? Curr Opin Pharmacol 2010;10:698–705.
[32] **Zhang J**, **Huang W**, Chua SS, Wei P, Moore DD. Modulation of acetaminophen-induced hepatotoxicity by the xenobiotic receptor CAR. Science 2002;298:422–424.
[33] Bhushan B, Borude P, Edwards G, Walesky C, Cleveland J, Li F, et al. Role of bile acids in liver injury and regeneration following acetaminophen overdose. Am J Pathol 2013;183:1518–1526.
[34] Snawder JE, Roe AL, Benson RW, Roberts DW. Loss of CYP2E1 and CYP1A2 activity as a function of acetaminophen dose: relation to toxicity. Biochem Biophys Res Commun 1994;203:532–539.
[35] Hinson JA, Roberts DW, James LP. Mechanisms of acetaminophen-induced liver necrosis. Handb Exp Pharmacol 2010;196:369–405.
[36] Arnaiz SL, Llesuy S, Cutrín JC, Boveris A. Oxidative stress by acute acetaminophen administration in mouse liver. Free Radic Biol Med 1995;19:303–310.
[37] Xie W, Barwick JL, Downes M, Blumberg B, Simon CM, Nelson MC, et al. Humanized xenobiotic response in mice expressing nuclear receptor SXR. Nature 2000;406:435–439.
[38] Gonzalez FJ. Cytochrome P450 humanised mice. Hum Genomics 2004;1(4):300–306.
[39] Carulli N, Manenti F, de Leon MP, Ferrari A, Salvioli G, Gallo M. Alteration of drug metabolism during cholestasis in man. Eur J Clin Invest 1975;5:455–462.